

Auxiliary Material of Lin, M., et al. (2012),
Transport of Asian ozone pollution into
surface air over the western United States in
spring, *J. Geophys. Res.*, 117, D00V07,
doi:10.1029/2011JD016961.

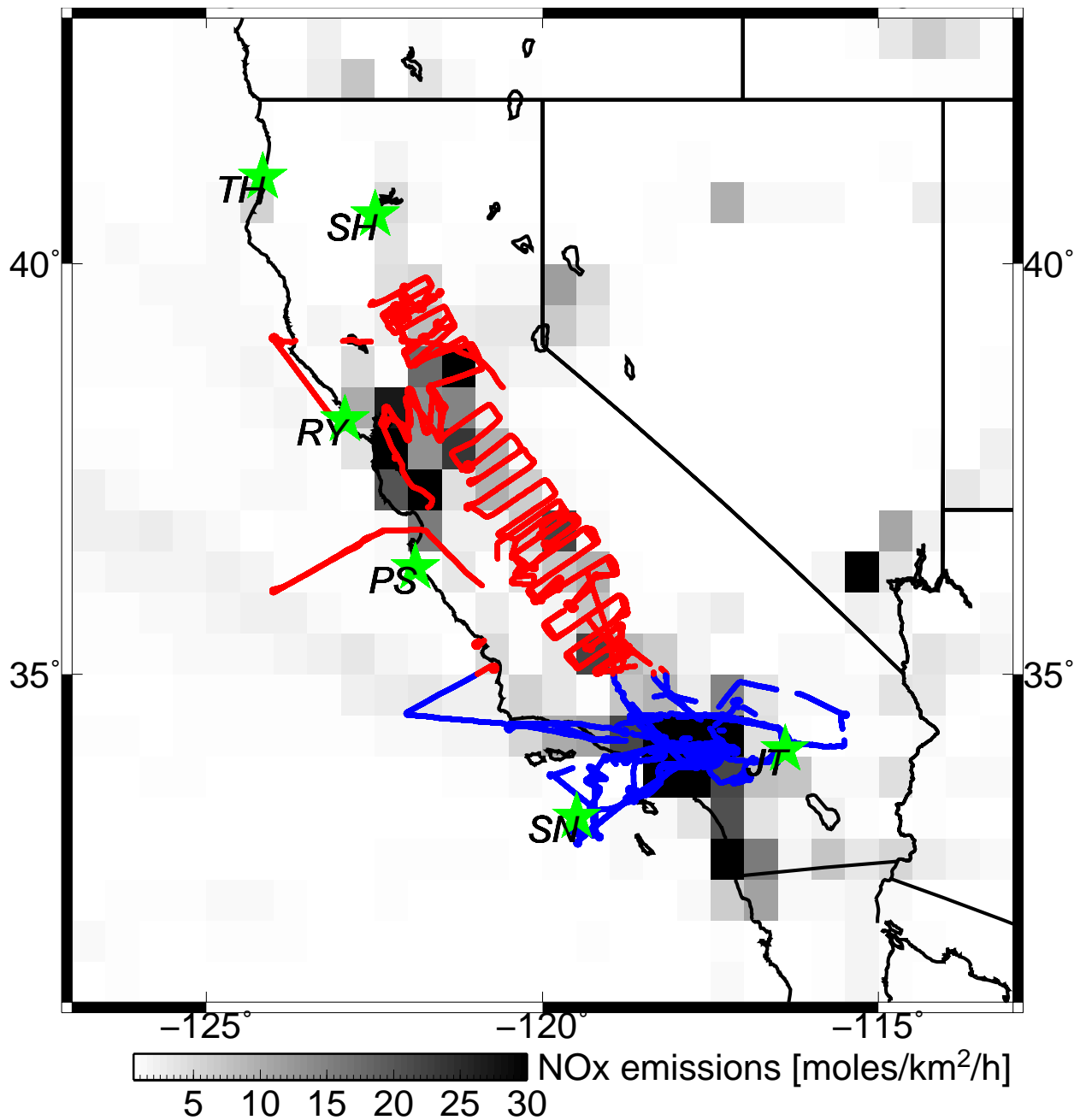


Figure S1. Locations of ozonesondes (green stars) and selected WP-3D daytime flight legs below 1.5 km over in the LA Basin (blue) and the Central Valley (red) of California during CalNex 2010.

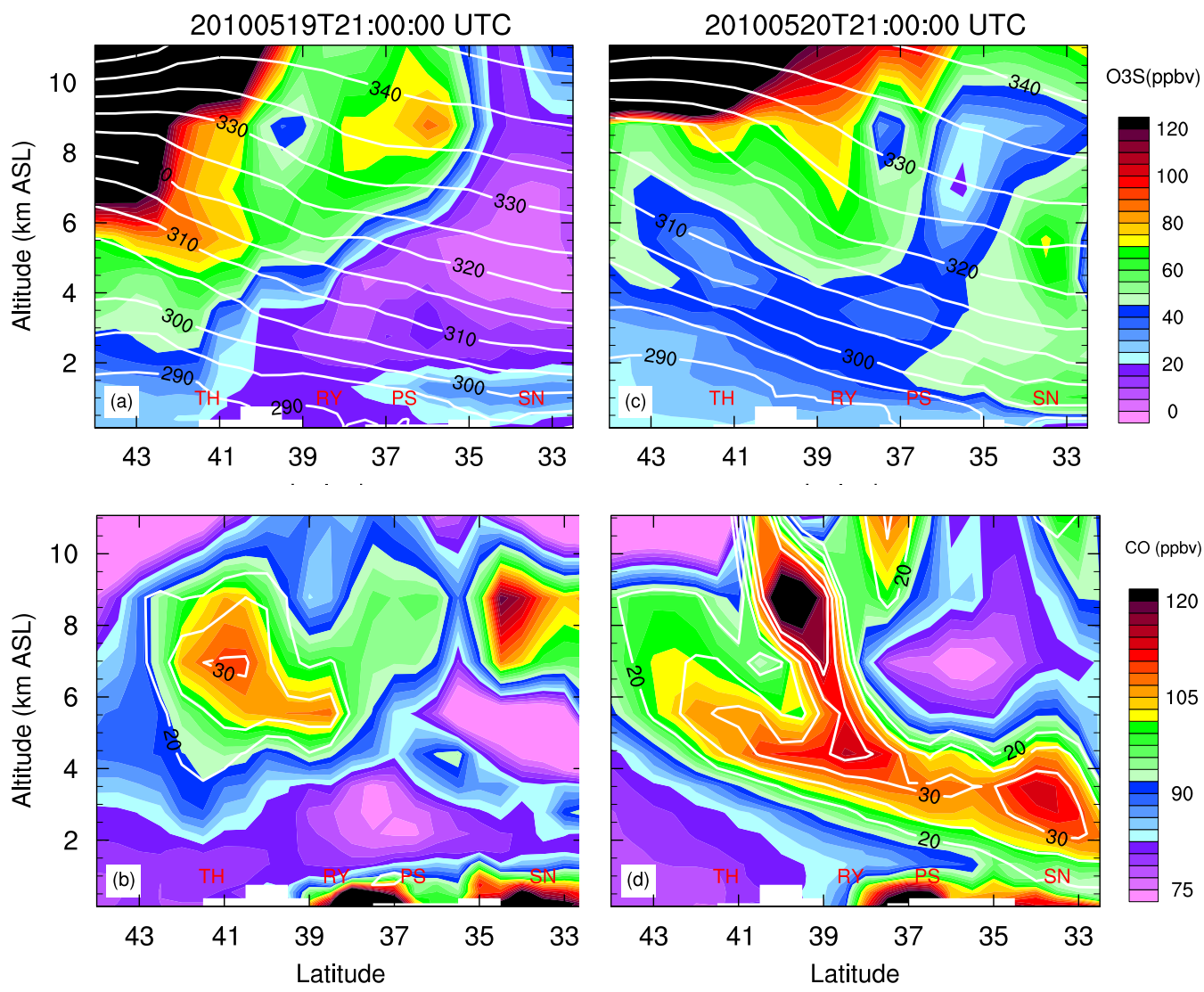


Figure S2. Vertical cross-section along California coast (thick black line in Fig.3e), Showing (top) simulated stratospheric ozone tracer (shading, Section 2.3) with isentropic surfaces on May 19-20, 2010 and (bottom) total CO (shading) with Asian CO (contours) as determined by the difference between the standard simulation and a sensitivity simulation with Asian anthropogenic emissions shut off. Letters in red denote locations of ozonesondes (Fig. S1).

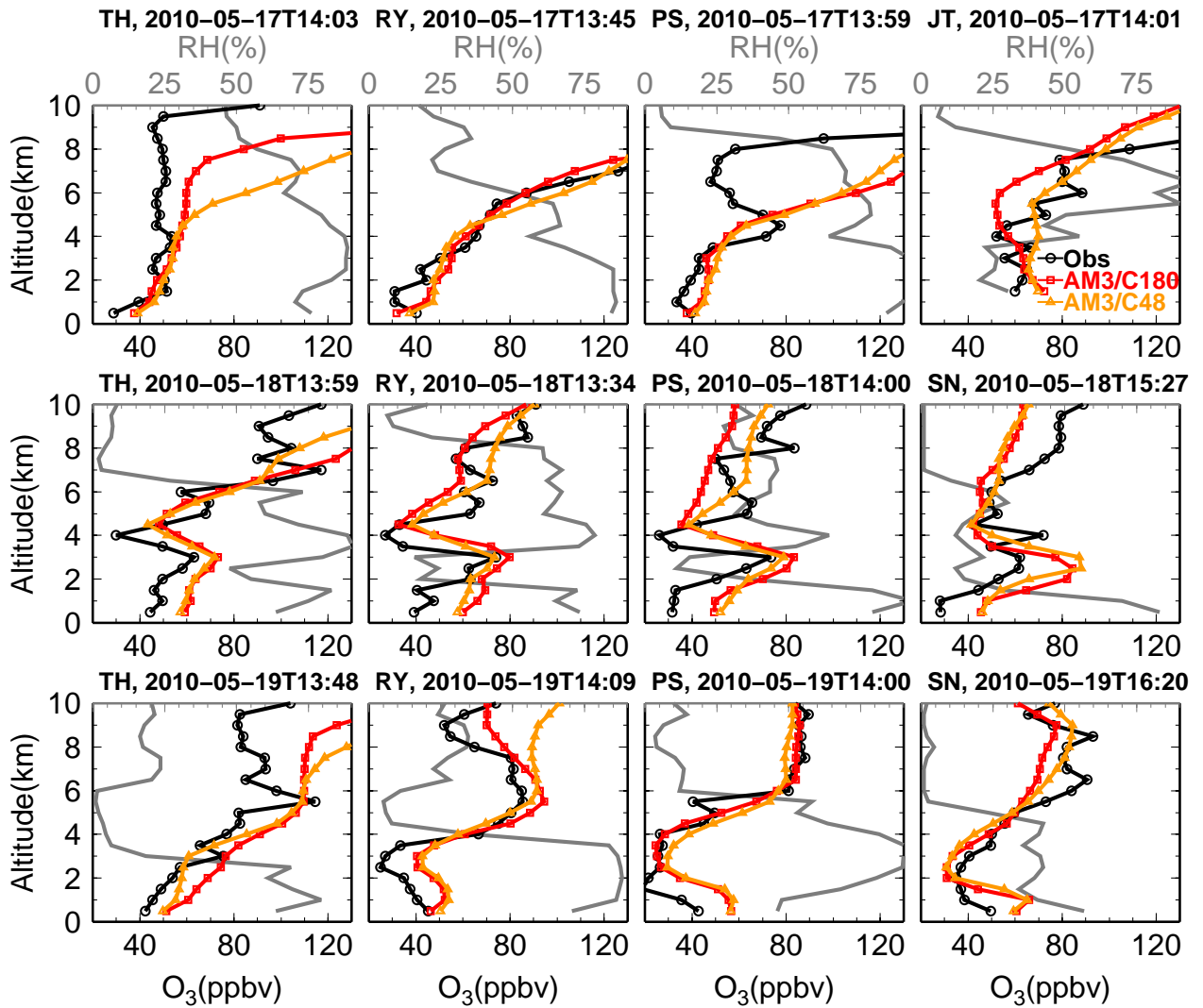


Figure S3. Comparison of AM3/C48 (~163-231 km, orange) and AM3/C180 (~43-62 km, red) O₃ vertical profiles with ozonesondes (black, locations shown in Fig. S1) in California during a stratospheric intrusion and Asian pollution event on 17-19 May 2010 (Section 3.1). Also shown is measured relative humidity (gray).

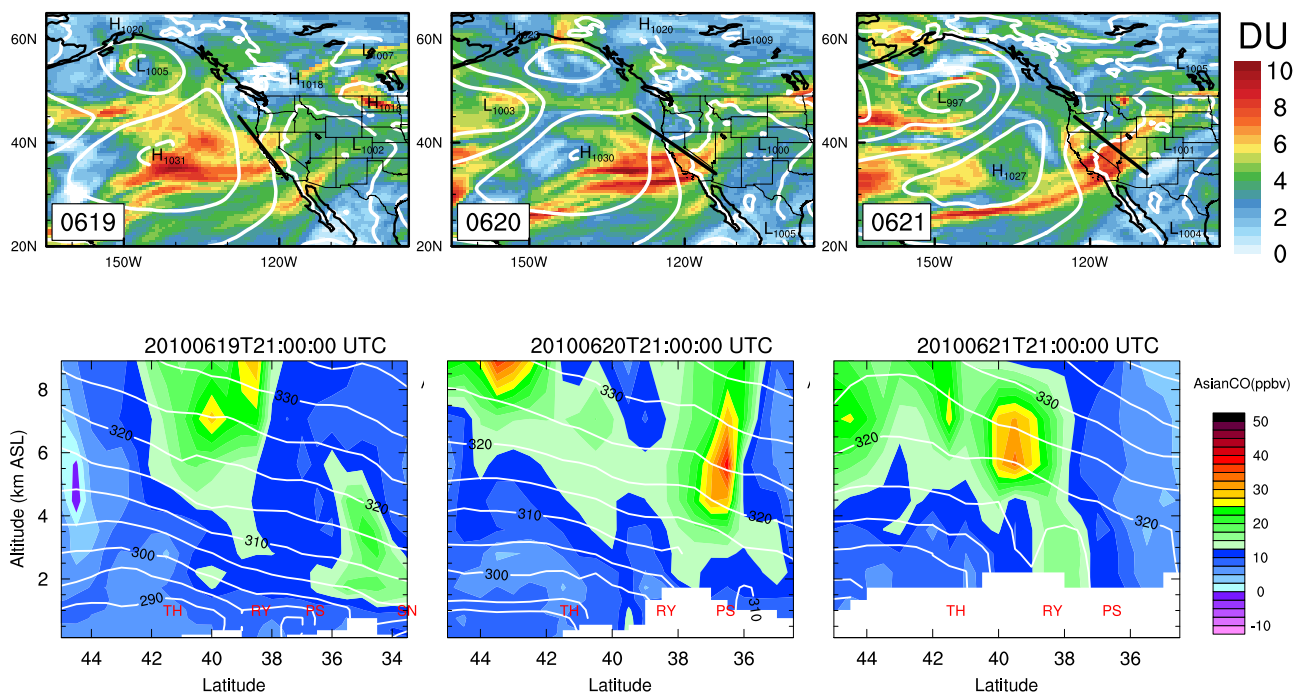


Figure S4. Propagation of Asian pollution from the North Pacific Ocean to the western USA from June 19-21, 2010 (Section 3.2). Shown are (top) Asian enhancements to daily mean tropospheric column ozone (shading) with sea level pressure (contours, hPa) and (bottom) subsidence of Asian CO (shading) along isentropic surfaces (contours, K) as air masses travel from north to south (thick black lines in the top panels)

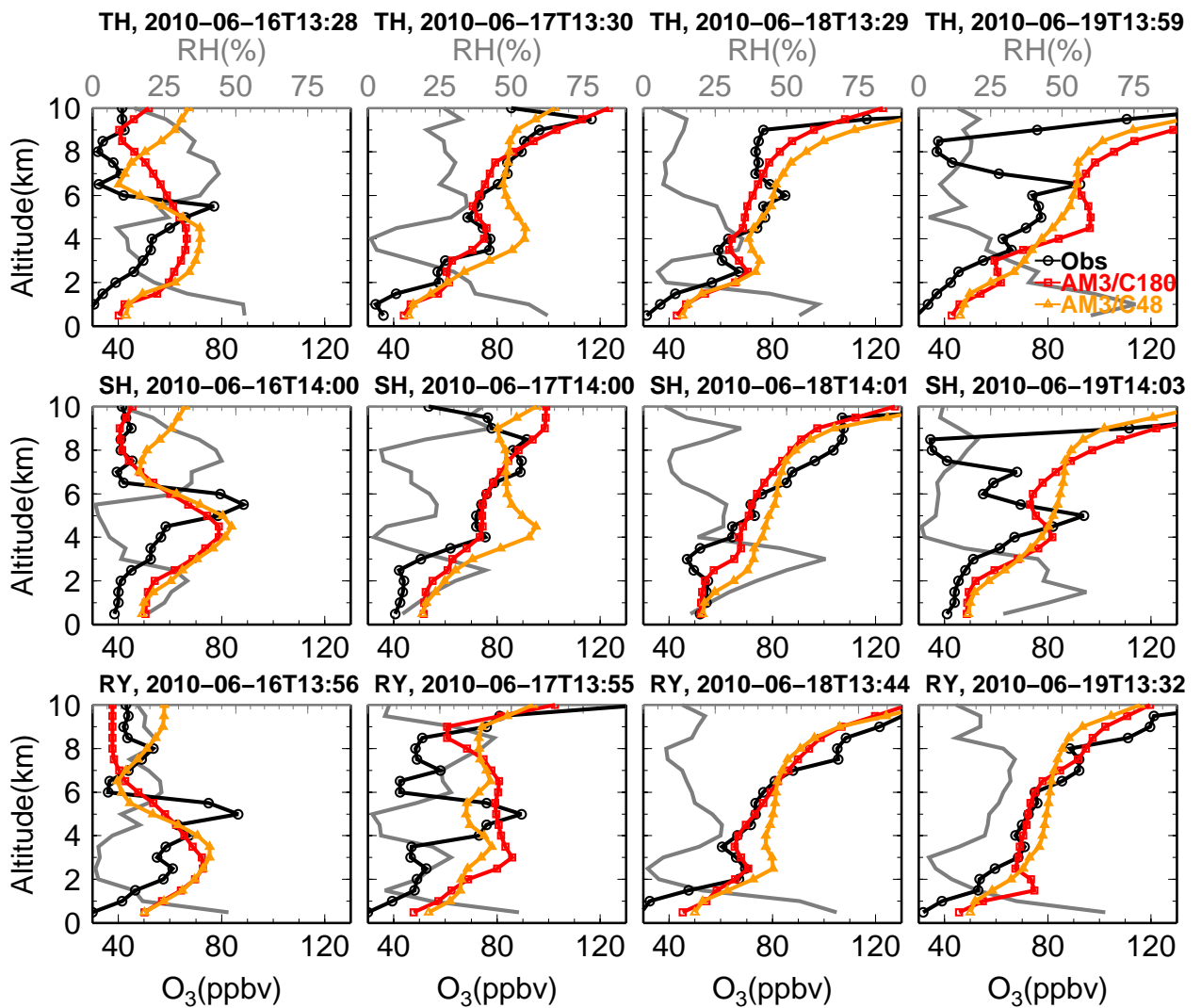


Figure S5. As in Figure S3, but for June 16-19, 2010 (Section 3.2).

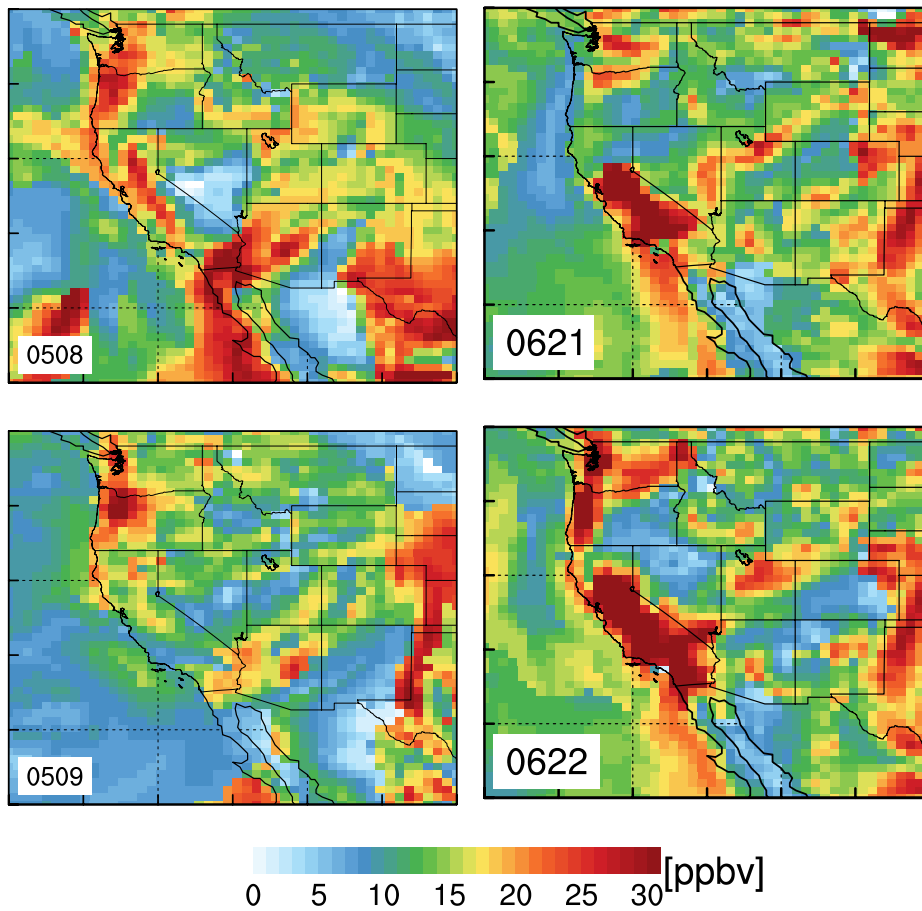


Figure S6. Contribution of North American anthropogenic emissions to MDA8 O₃ in the model surface layer on May 8-9 and June 21-22, 2010, as determined by the difference between the base simulation and a sensitivity simulation with North American anthropogenic emissions turned off.

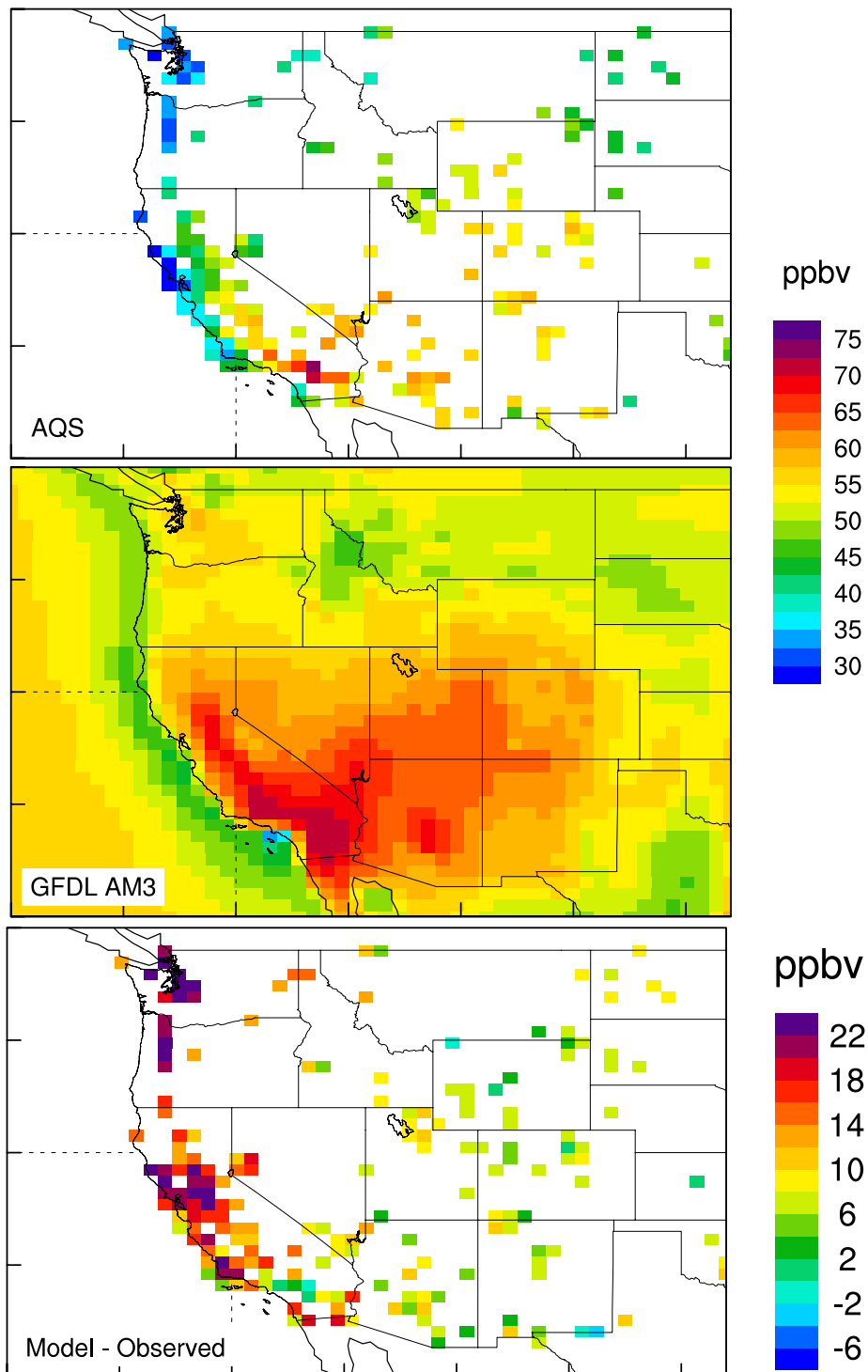


Figure S7. Mean MDA8 O₃ in surface air over the western U.S. in May-June 2010 showing (top) the AQS observations, (middle) the GFDL AM3 model surface layer, and (bottom) the difference between the AM3 model and AQS observations.

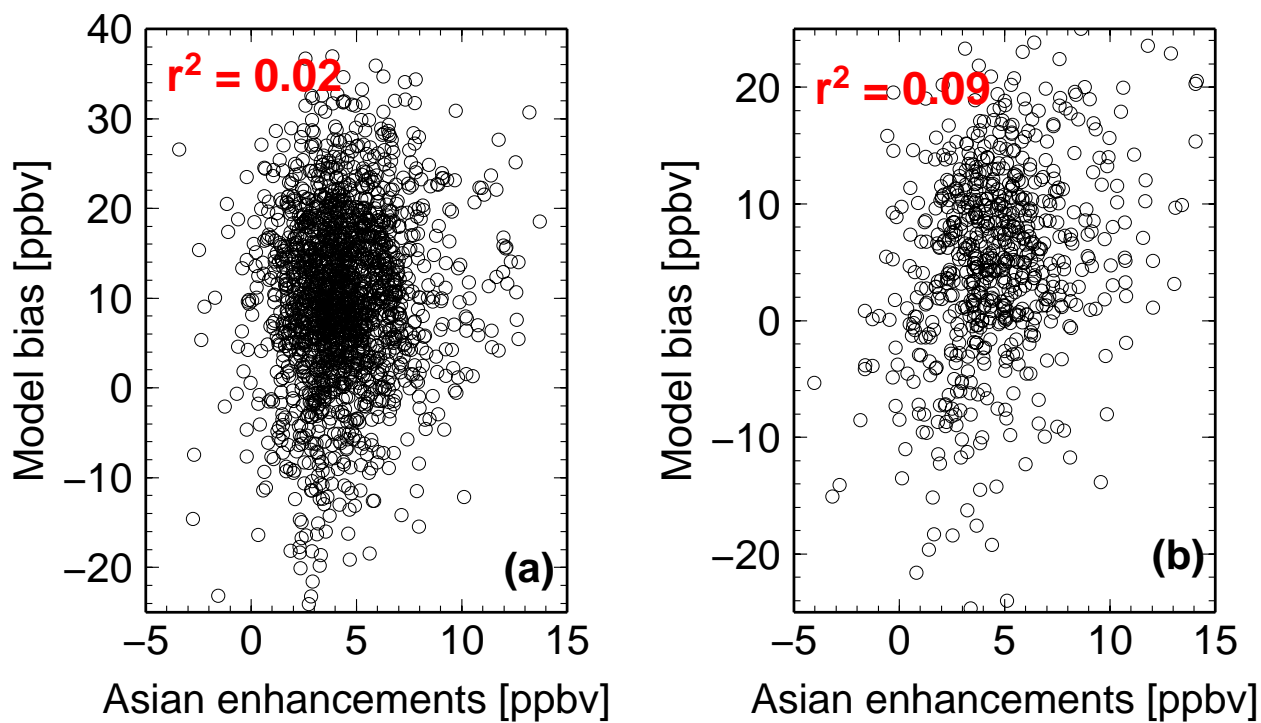


Figure S8. Scatter plot of Asian enhancements vs. model biases in MDA8 O₃, sampled in the model surface layer, (a) for all AQS sites in the southwest U.S. (box in Fig.12a) and (b) for CASTNet high-elevation sites (white symbols in Fig.12b).

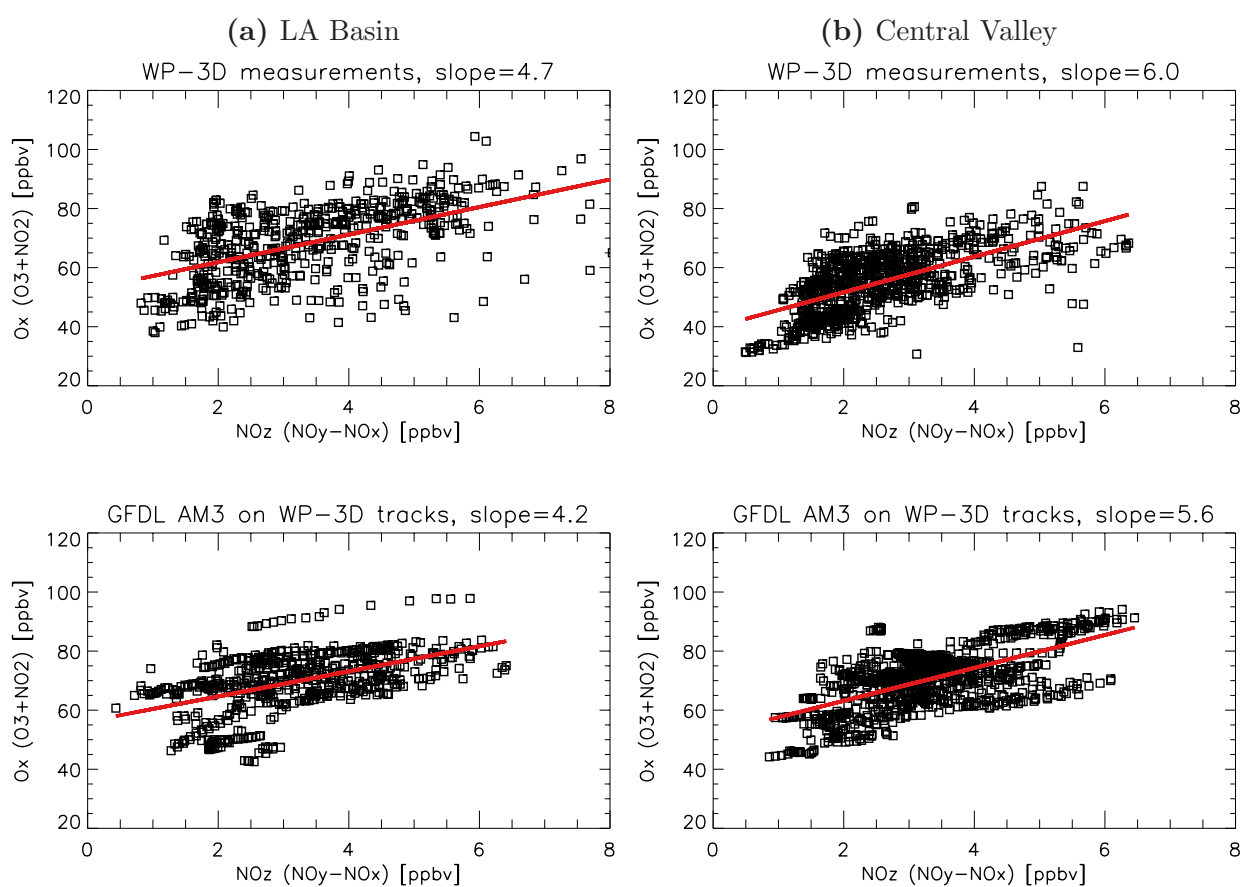


Figure S9. Ozone production efficiency: O_x vs. NO_z from WP-3D daytime measurements and results from the GFDL AM3 model sampled at flight tracks below 1.5 km over (a) the LA Basin and (b) the Central Valley. Only flight legs below 1.5 km (auxiliary Fig.S1) and points where NO_y is between 2 and 10 ppbv are included, so as to filter out fresh plumes and very aged air, retaining only moderately polluted air masses. The slope from the linear regression of O_x to NO_z is given.

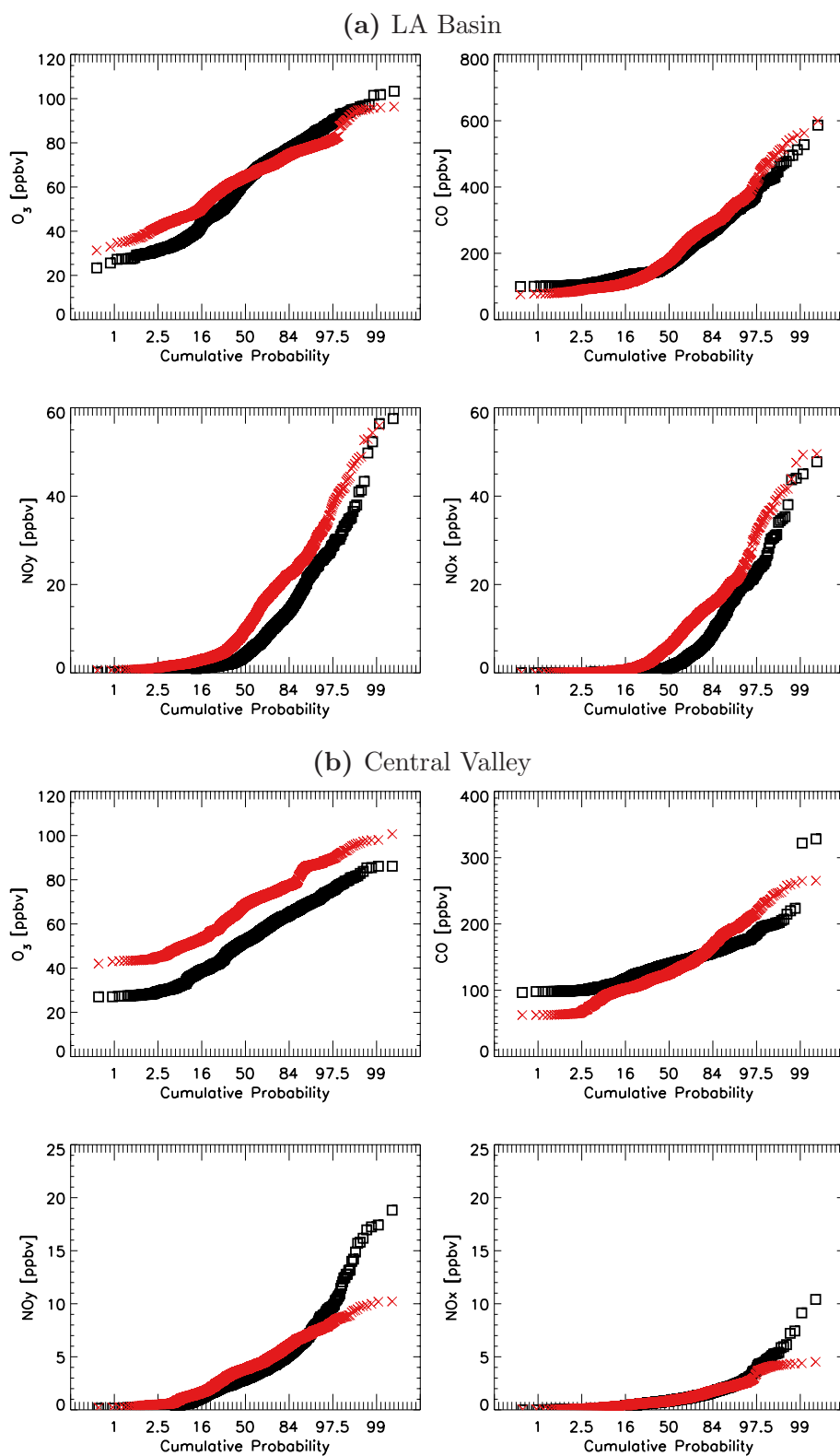


Figure S10. Comparison of cumulative probability distributions of O_3 , CO, NO_y , and NO_x from WP-3D measurements (black) and results from AM3/C180 (red) sampled at WP-3D flight tracks below 1.5 km over (a) the LA Basin and (b) the Central Valley shown in Fig. S1

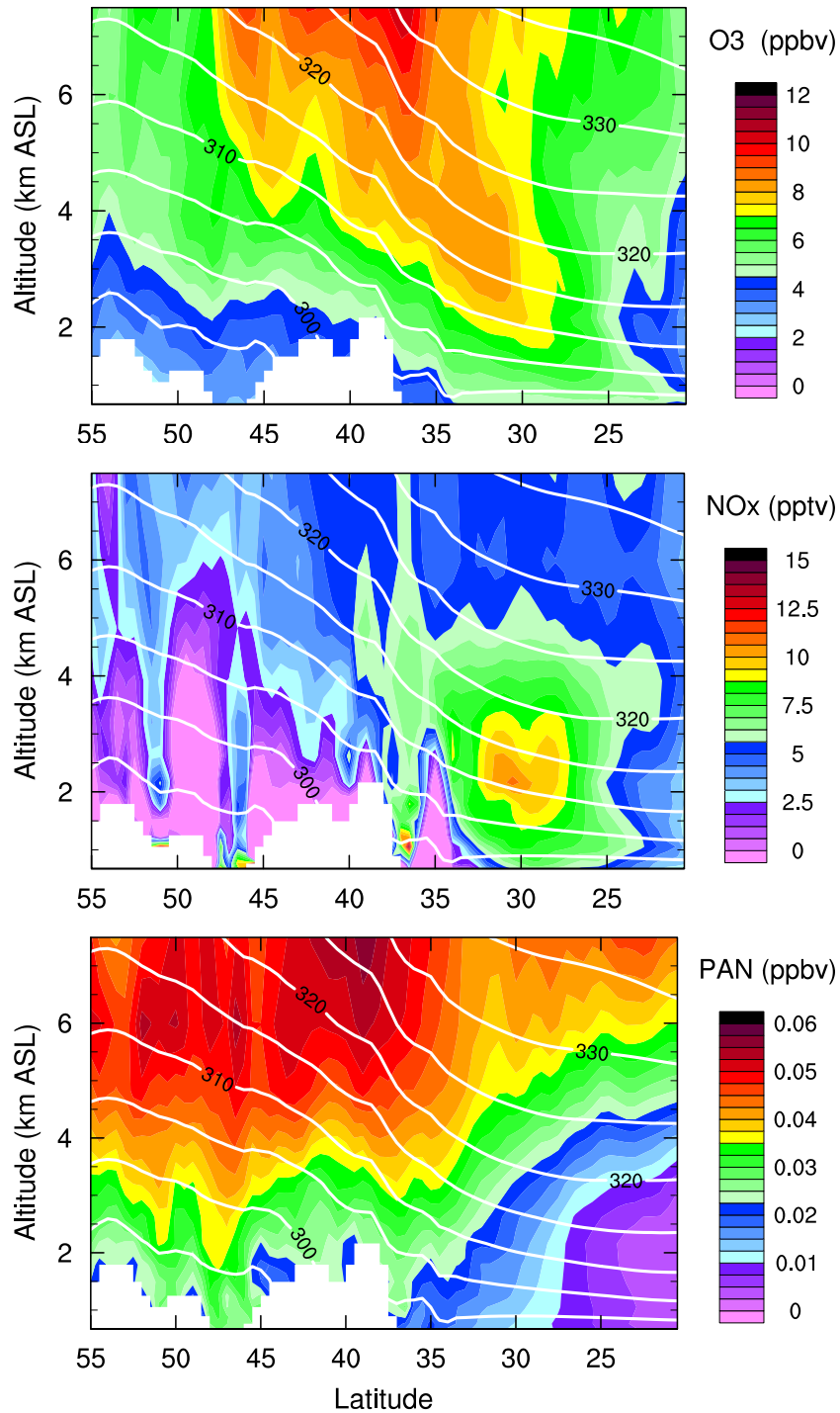


Figure S11. May-June 2010 mean vertical distributions of Asian anthropogenic enhancements to O_3 , NO_x , and PAN with isentropic surfaces (contours, K) along a north-south transect at $120^\circ W$. Note that the unit for Asian NO_x is pptv.